J. Environ. Nanotechnol.
Volume 6, No.3(2017) pp. 94-102
ISSN (Print): 2279-0748
ISSN (Online): 2319-5541
doi:10.13074/jent.2017.09.173273

Synthesis, Structural and Optical Characterization of TiO_2 Nanoparticles and its Assessment to Cytotoxicity Activity

K. Manikandan[1*], A. JafarAhamed[2], G. M. Brahmanandhan[3]

[*1]*Department of Chemistry, Velalar College of Engineering and Technology, (Autonomous), Erode, India.*
[2]*Department of Chemistry, Jamal Mohamed College, (Autonomous), Trichy, India.*
[3]*Department of Nanomaterials, Kattankulathur, Chennai, India.*

Received: 02.01.2017 Accepted: 28.01.2017

Abstract

In this research work,TiO_2 nanoparticles was synthesised by solgel method using titanium (IV) isopropoxide and calcinated at 500° C, 600° C and 700° C for five hours. The synthesised nanoparticles are characterized by using X-ray Diffraction studies (XRD), Field Emission Scanning Electron Microscopy (FESEM), Energy Dispersive X-ray Spectroscopy (EDXA), UV-Vis Diffuse Reflectance Spectroscopy (UV-Vis), Photoluminescence Spectra (PL), High Resolution Transmission Spectroscope (HRTEM) and Fourier Transform Infra Red Spectroscopy (FTIR). The synthesized nanoparticle of TiO_2 calcinated at 500° C and 600° C for 5 h shows anatase nature crystal structure and temperature increased to 700° C, they undergo structural changes to rutile structure at the same duration of calcination. Average crystallite size can be determined by Debye-Scherrer formula for synthesized nanoparticles shows the particle sizes range from 30 nm to 47 nm. EDXA analysis confirms no impurities present in the sample. The band gap value decreases from 2.95 eV to 2.79 eV when calcination temperature increases in the UV-Visible analysis. The photoluminescence study of TiO_2 shows the direct recombination between electrons in the conduction band and holes in the valence band. FTIR analysis shows the bending and stretching mode of Ti-O-Ti. HRTEM of TiO_2 nanoparticles shows nearly spherical with approximately particles size of 35 nm to 50 nm. The cytotoxicity activity of TiO_2 nanoparticles calcinated at 500° C, 600° C and 700° C has been explored.

Key words: *Cytotoxicity activity; HRTEM; SEM; Solgel method; TiO2; XRD.*

1. INTRODUCTION

TiO_2 is naturally occurring in oxide of Titanium. The high refractive index, non-toxic property, high chemical stability are some of the important properties of titanium dioxide and it has relatively low-cost of production (Kamat *et al.* 1999; Rammal *et al.* coworkers 2002; Rubing Zhang *et al.* 2004;).Generally, Titanium dioxide has been used in paints as a pigment and filler (Krishnamurthy Prasad *et al.* 2010), ointments, toothpaste etc (Shuai Yuan*et al.* 2005; Juergen, Braun *et al.* 1992; Zallen and Moret 2006;). Figure 1 shows the three forms TiO_2, rutile (Tetragonal, a=b=3.78A°, c=9.5A°), anatase (Tetragonal, a=b=3.78A°, c=9.5A°) and brookite (Rhombohedral, a=5.43A°, b=9.16A°, c=5.13A°) forms. All crystalline forms TiO_2 consist of $[TiO_6]^{2-}$ octahedral structure. Anatase form of TiO_2 possess a wider optical band gap (3.2 eV), a higher fermi level, a smaller electron effective mass, and high mobility of charge carriers. But rutile phase is highly stable phase at high temperature (Mogyorosi *et al.* 2003.). The edges and corners of this structure have different manners, but the overall stoichiometry as TiO_2 (Mark *et al.*1983; Weast *et al.*1984;). Anatase phase has changed to rutile phase is usually occurs at 600° C to 700° C (Czanderna *et al.* 1958; Yoganarasimhan and C.N.R.Rao1962). This phase transition to rutile is non-reversible. Because, rutile form has greater thermodynamic stability compared to anatase phase (Reidy *et al.* 2006. Navrotsky and Kleppla). A nanoparticle of titanium dioxide plays an important role in the fields of photo catalyst material for degradation of organic contaminants (Desong Wang *et al.* 2011) and as a self disinfecting material for surface coating in many applications. It is used in environmental purification, photo-electric chemical conversions in solar cells (Alam Khan *et al.* 2010), electronic devices, photo electrodes and gas sensors. The properties of Titanium dioxide such as photo induced super-hydrophobicity, nontoxicity and antifogging effect have been used in removing bacteria and harmful organic materials from water and air. The size, the crystalline structure, and the morphology of the TiO_2 nanoparticles strongly affect

K. Manikandan
email: chemmani03@gmail.com

the performance of the TiO_2 (Kavan *et al.*1996; Krol *et al.*1997; Hadjipanayis *et al.* 1994;). So, there are variety of researchers focusing on the preparation of nanoparticles of TiO_2 using ethanol along with different acid and bases.

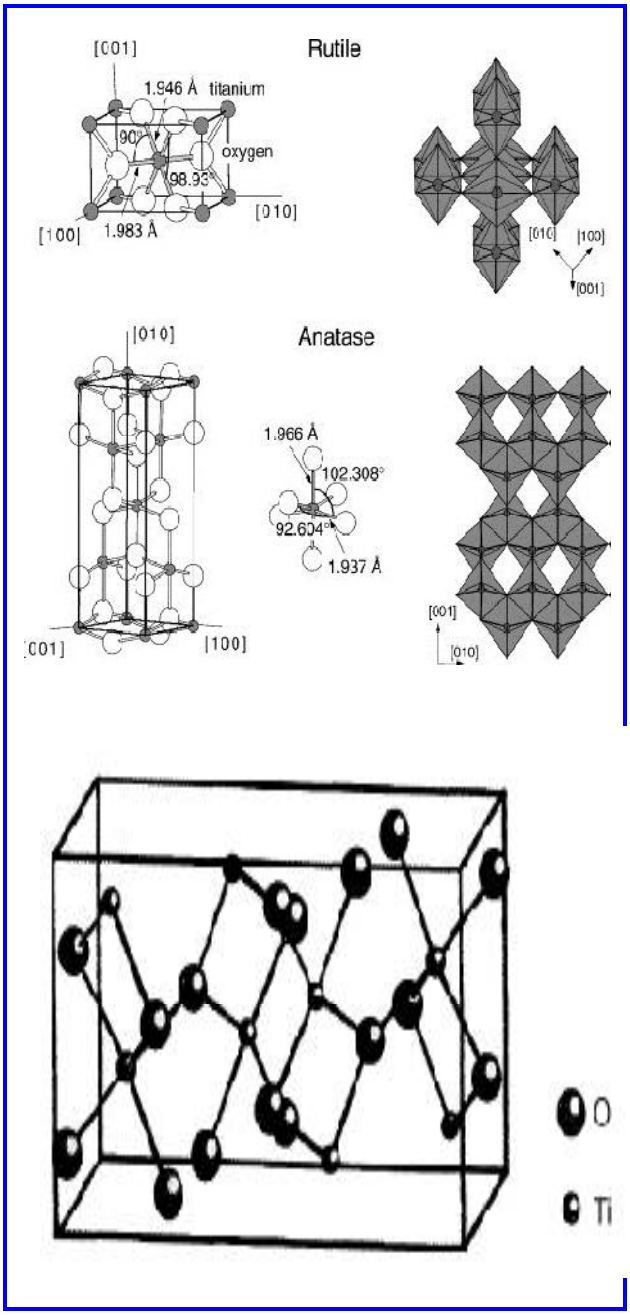

Fig. 1: Crystal structures of TiO_2 rutile, anatase and brookite phase

In this work, an easy and new way of synthesizing nano particles of TiO_2 using titanium (IV) isopropoxide, ethanol and hydroxylamine hydrochloride has been discussed. Synthesised TiO_2 nanoparticles have been employed for the characterization such as X-ray Diffraction (XRD), Field Emission Scanning Electron Microscopy (FESEM), Energy Dispersive X-ray Spectroscopy (EDXA), Ultraviolet-Visible Diffuse Reflectance Spectroscopy (UV), Photoluminescence Analysis (PL), Fourier Transform Infra Red Spectroscopy (FT-IR), and High Resolution Transmission Electron Microscopy (HRTEM).

2. EXPERMENTAL METHODS

2.1 Material

Titanium isopropoxide (Sigma-Aldrich > 97 % pure), ethanol (Hayman (German) 99.99 % pure), hydroxylamine hydrochloride (Sigma-Aldrich, 99 % pure) were used as precursors and is used without any further purification. Doubly distilled water was used for the whole synthesis process.

2.2 Physicochemical characterization

The X-ray diffraction pattern analysis for TiO_2 nanoparticles was recorded by Lab X XRD6000 Shimadzu model with Cu-Ka radiation. The structure and morphology of the nanoparticles were investigated by Field Emission Scanning Electron Microscope (FESEM) using FEI Quanta FEG 200-High Resolution Scanning Electron Microscope. The absorption spectra and optical band gap of the TiO_2 nanoparticles samples were measured by using UV-Vis spectrophotometer (JASCO U-670 Spectrometer) and the alcohol as a solvent. The spectrum was recorded between 200-800 nm. A Photoluminescence spectrum was recorded between 370-770 nm and it was carried out by using Horiba Jobnyvon model spectrophotometer and the alcohol is used a solvent. FTIR absorption spectrum was recorded by JASCOFP8200 spectrophotometer. The particle size and lattice structure of the individual crystal was visualised by using High Resolution Transmission Electron Microscopy JE2100 (JEOL-200KV, LB6 filament) and EDXA analysis was carriedout to find the composition of TiO_2 samples by using the detector attached with the same instrument.

2.3 Synthesis of pure TiO_2 nanoparticles

Aqueous solution of titanium (IV) isopropoxide was used as starting material. Solgel is the most simple and sophisticated method proposed by Byun *et al.* 2000 among the various methods for producing nanoparticles. The sol was prepared by mixing titanium iso propxide and ethanol having molar ratio 1:8 and dissolved in 1000 ml of deionised water at room temperature. Hydroxylamine hydrochloride 0.694 g was dissolved in 100 ml of deionised water and added gradually to the titanium iso propoxide sol. After 45 min of vigorous stirring, the suspension was centrifuged and precipitate obtained was washed with single step deionised water. After centrifugation, the precipitate was dried at 105° C till the samples were converted into dry powder. The prepared samples were calcinated at

500° C, 600° C and 700° C for five hours at a constant temperature of 2° C/min.

2.3 Cytotoxicity activity of TiO_2

2.3.1 Methodology

2.3.1.1 Cell line

The human embryonic kidney cell line (HEK 293) was obtained from National Centre for Cell Science (NCCS), Pune and grown in Eagles Minimum Essential Medium containing 10 % fetal bovine serum (FBS). The cells were maintained at 37° C, 5 % CO_2, 95 % air and 100 % relative humidity. Maintenance cultures were passaged weekly, and the culture medium was changed twice a week.

2.3.1.2 In vitro cytotoxic activities for TiO_2 nanoparticles

The monolayer cells were detached with trypsin-ethylenediamine tetra acetic acid (EDTA) to make single cell suspensions and viable cells were counted using a hemocytometer and diluted with medium containing 5 % FBS to give final density of $1x10^5$ cells/ml. One hundred microlitres per well of cell suspension were seeded into 96-well plates at plating density of 10,000 cells/well and incubated to allow for cell attachment at 37° C, 5 % CO_2, 95 % air and 100 % relative humidity. After 24 h the cells were treated with serial concentrations of the test samples. They were initially dispersed in phosphate buffered saline (PBS) and an aliquot of the sample solution was diluted to twice the desired final maximum test concentration with serum free medium. Additional four serial dilutions were made to provide a total of five sample concentrations (0.25 µg, 2.5 µg, 25 µg, 50 µg, and 100 µg/ml). Aliquots of 100 µl of these different sample dilutions were added to the appropriate wells already containing 100 µl of medium, resulting in the required final sample concentrations. Following sample addition, the plates were incubated for an additional 48 h at 37° C, 5 % CO_2, 95 % air and 100 % relative humidity. The medium containing without samples were served as control and triplicate was maintained for all concentrations.

2.3.1.2 MTT assay

3-[4, 5-dimethylthiazol-2-yl]2,5-diphenyltetrazolium bromide (MTT) is a yellow water soluble tetrazolium salt. A mitochondrial enzyme in living cells, succinate-dehydrogenase, cleaves the tetrazolium ring, converting the MTT to an insoluble purple formazan. Therefore, the amount of formazan produced is directly proportional to the number of viable cells.

After 48 hours of incubation, 15 µl of MTT (5 mg/ml) in phosphate buffered saline (PBS) was added to each well and incubated at 37° C for 4 h. The medium with MTT was then flicked off and the formed formazan crystals were solubilised in 100 µl of DMSO and then measured the absorbance at 570 nm using micro plate reader.

- The percentage cell growth was then calculated with respect to control as follows

  % Cell growth = [A] Test / [A]control x 100

- The % cell inhibition was determined using the following formula.

  % Cell Inhibition=100-Abs(sample)/Abs(control)100.

3 RESULTS & DISCUSSION

3.1 X-Ray diffraction study (XRD)

The XRD patterns of TiO_2 samples calcinated at 500° C, 600° C and 700° C shown in the figure 2. It is clear that the TiO_2 present in its anatase form at 500° C, 600° C. Phase transformation to rutile form is identified in XRD results when calcination temperature increased to 700° C. The obtained 2θ values and corresponding (hkl) planes are 25.3° (101), 38° (004), 48° (200), 54° (105), 63° (204), 69.23° (116), 70.89° (220), 75.38° (215) respectively for TiO_2 nanoparticles calcinated at 500°C, 600°C (JCPDS Card No.21-1272).When calcination temperature increases to 700° C, shows the shifting of peaks at 27.3°, 36°, 41.2°, 54°,69° (in figure 2(c) corresponding to the hkl values (110), (101), (111), (210), (112) (JCPDS Card No.88-1175) indicate that phase has been changed from anatase into rutile. The preferred peak for 2θ value 25.3° was observed with corresponding plane (101), which is the strongest peak among other peaks for all the TiO_2 nanoparticles calcinated at temperatures of 500° C, 600° C which is not available when the calcination temperature increased to 700° C, supports the changes in phase from anatase to rutile. The peaks of the graph are in good agreement with the literature report by Akarsu *et al.* 2006.The average size of the particles was calculated using Debye-Scherrer's formula.

$$\text{Crystallite size} = 0.9\lambda / \beta \cos \theta,$$

Where β is the full width at half-maximum ($FWHM_{hkl}$) of an hkl peak at 2 θ value,

θ is the half of the scattering angle.

The calculated particle size of TiO_2 nanoparticles is approximately about 30, 37 and 47nm respectively.

3.2 Field Emission Scanning Electron Microscope (FESEM)

FESEM images provide information about the surface morphology. From the images shown in the figure 3, confirms the grains of nanoparticles of TiO_2 appear to be nearly spherical and uniform sized particles and coherent together. However, the individual spherical particles are not clearly seen due to the nano-clusters formed during the growth.

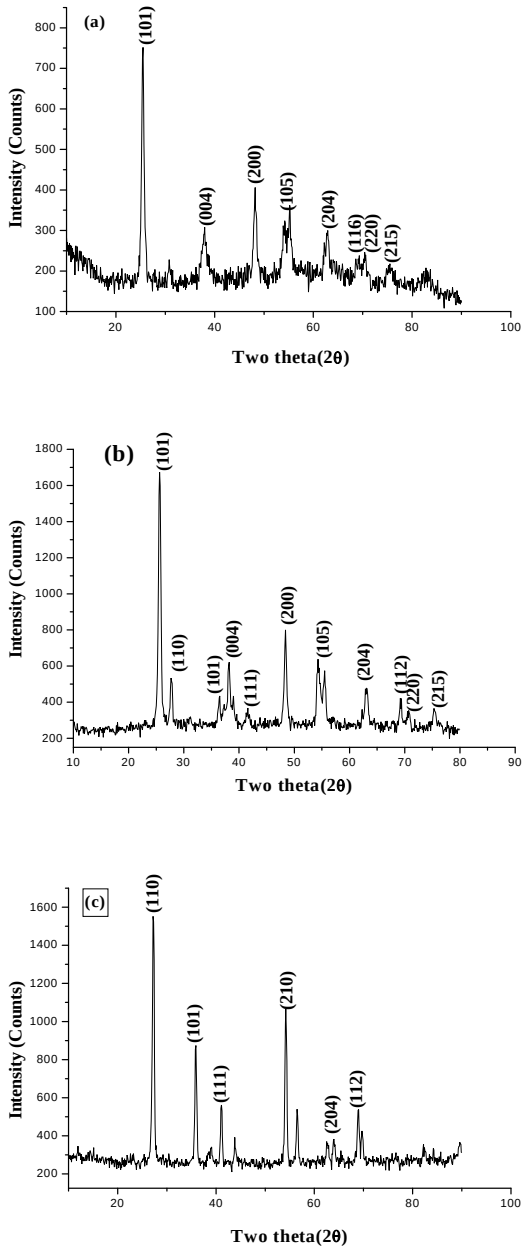

Fig. 2: XRD patterns of TiO_2 nanoparticles calcinated at (a) 500° C (b) 600° C (c) 700° C

3.3 Energy Dispersive Analysis by X-Rays (EDXA)

EDXA is used for chemical composition of a material. Figure 4 shows the EDXA of TiO_2 nanoparticles which contains only peaks of titanium and oxygen. From the figure 4 (a, b and c), it is clear that TiO_2 is free from impurities.

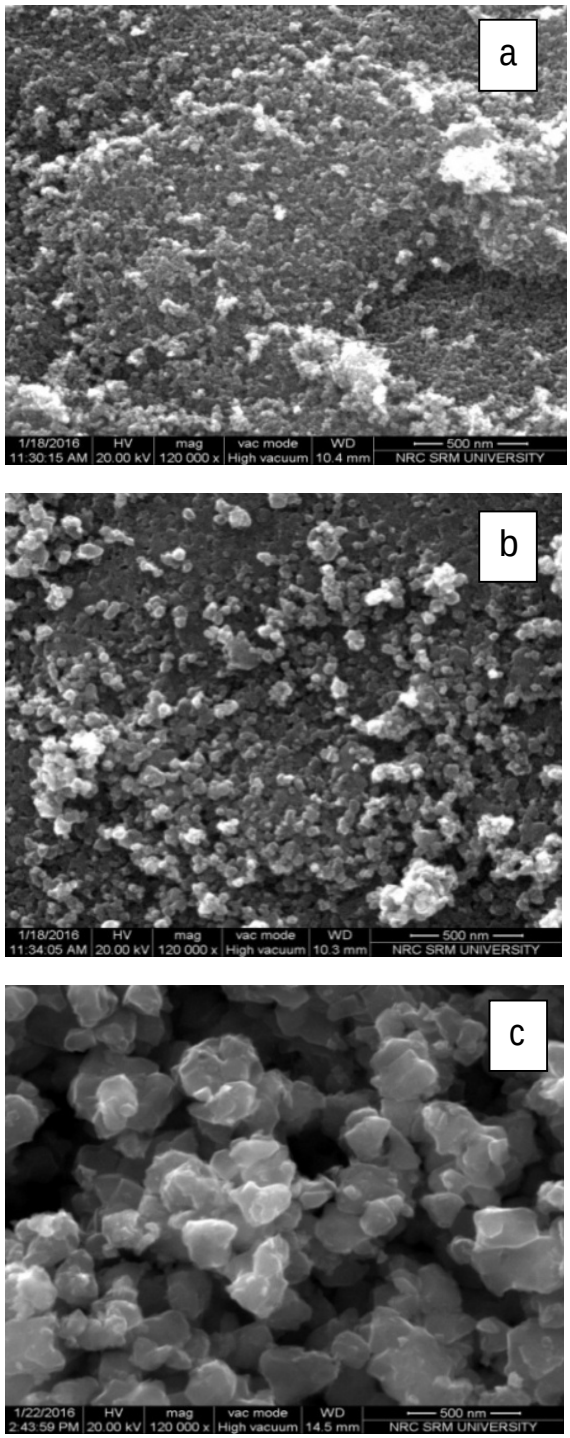

Fig. 3: FESEM images of TiO_2 nanoparticles calcinated at (a) 500° C (b) 600° C (c) 700° C

3.4 UV–Visible diffuse reflectance spectroscopy (UV-Vis)

Figure 5 shows the UV-Visible spectra of the TiO_2 at different temperatures of 500°C, 600° C and 700° C. It shows the absorbance can be decreased at wavelength after 350 nm for intrinsic band gap absorbance of TiO_2 due to electron transition from the valence band to the conduction band. Red shift was observed for TiO_2 nanoparticles in the absorbance edge is due to this change in surface morphology, particles size (Senthil *et al.*2014) and also variation in the absorbance may be due to variation in the annealing temperature (Elangovan *et al.* 2015). The band gap is determined by analysing the absorption of incident light by the nanomaterials. The band gap energy can be determined by extrapolation of the absorption edge onto the x-axis and by using the Planck's equation

$$E_g = h\ C/\lambda$$

Where, E_g is the energy gap of pure TiO_2 at absorption wavelength λ, h is the Planck's constant, C is the velocity of light.

The calculated band gap value for TiO_2 was calcinated at 500° C, 600° C and 700° C are 2.95 eV, 2,86 eV and 2.79 eV respectively. The band gap energy decreased with the increase of calcinated temperature. At higher calcinated temperature 700° C shows lowest band gap (2.79) is due to rutile phase is formed which has a bigger particle size (Swapan *et al.* 2010).

3.5 Photoluminescence study (PL)

The photoluminescence spectrum was recorded for TiO_2 nanoparticles which are shown in figure 6. The emission of first peak in the photoluminescence spectra obtained at three calcination temperature of TiO_2 nanoparticles between 360 nm to 420 nm corresponds to the direct recombination between electrons in the conduction band and holes in the valence band (Liqiang *et al.* 2004). The presence of emission peaks in the visible region is due to the presence of defect levels below the conduction band. Similar peak has been observed in earlier work on TiO_2 nano particles (Vijayalakshmi and Rajendran 2012).

The presence of broad peak in the visible region of PL spectrum indicates the presence of defect levels below the conduction band and the electronic transition takes place by defect levels such as oxygen vacancies in the band gap (Zhao *et al.* 2007) .

3.6 Fourier transform infrared spectroscopy (FTIR)

A FTIR spectrum is used to analyses the functional groups of titanium dioxide nanoparticles. In FTIR spectrum of titanium dioxide nanoparticles in which the peaks stretching vibration at 3523 cm^{-1} and bending vibration 1722.43 cm^{-1} in the spectra are due to –OH group shown in Figure 7. It shows peaks at 433 cm^{-1}, 514 cm^{-1} to 700 cm^{-1} for bending and stretching mode of Ti-O-Ti. The samples after calcinations show that there was no peak at 2800 cm^{-1} which means that all organic compounds were removed from the titanium dioxide nanoparticles.

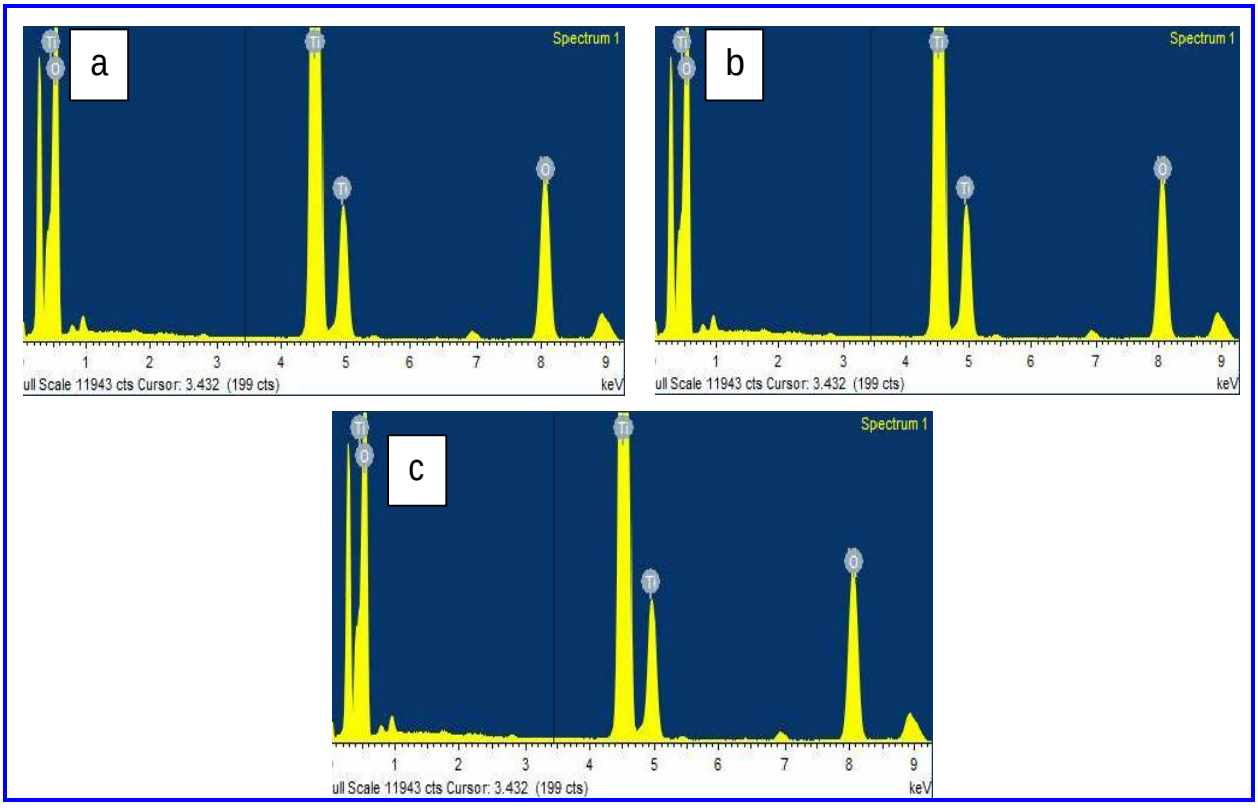

Fig. 4: EDXA pattern of TiO_2 nanoparticles calcinated at (a) 500° C (b) 600° C (c) 700° C

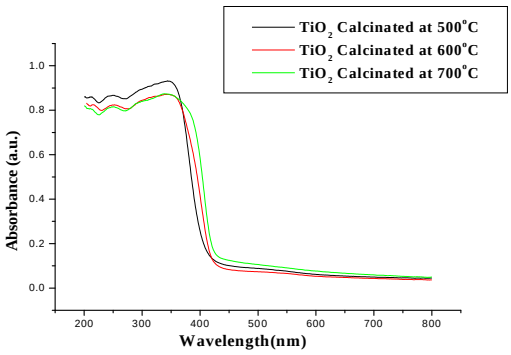

Fig. 5: UV-Vis diffuse reflectance spectra of TiO_2 nanoparticles calcinated at 500° C, 600° C and 700° C

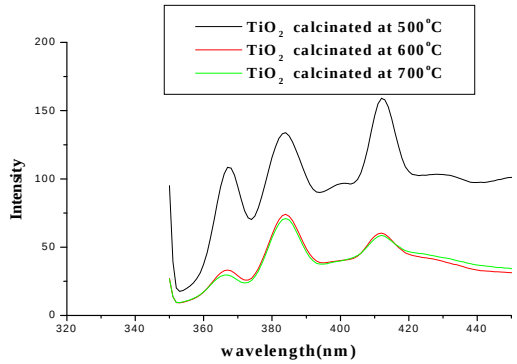

Fig. 6: Photoluminescence spectra of TiO_2 nanoparticles calcinated at 500° C, 600° C and 700° C

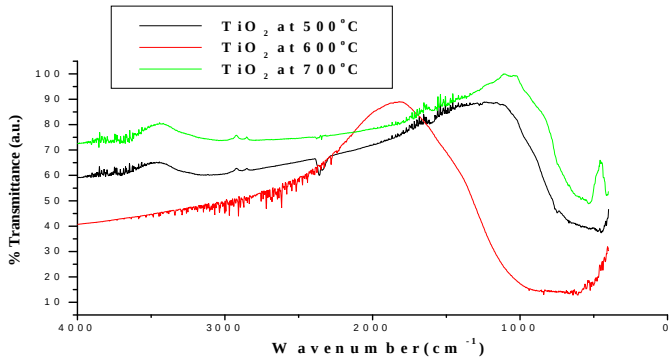

Fig. 7: FTIR spectra of TiO_2 nanoparticles calcinated at 500° C, 600° C, and 700° C

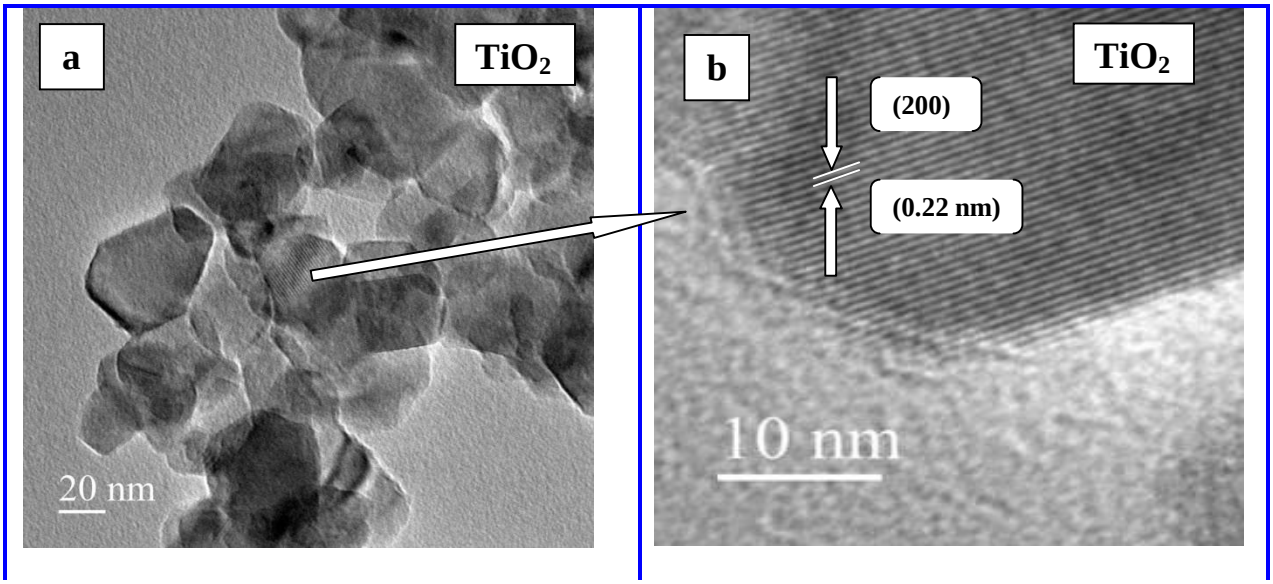

Fig. 8: High Resolution Transmission Electron Microscope image of TiO_2 nanoparticles prepared by sol-gel method

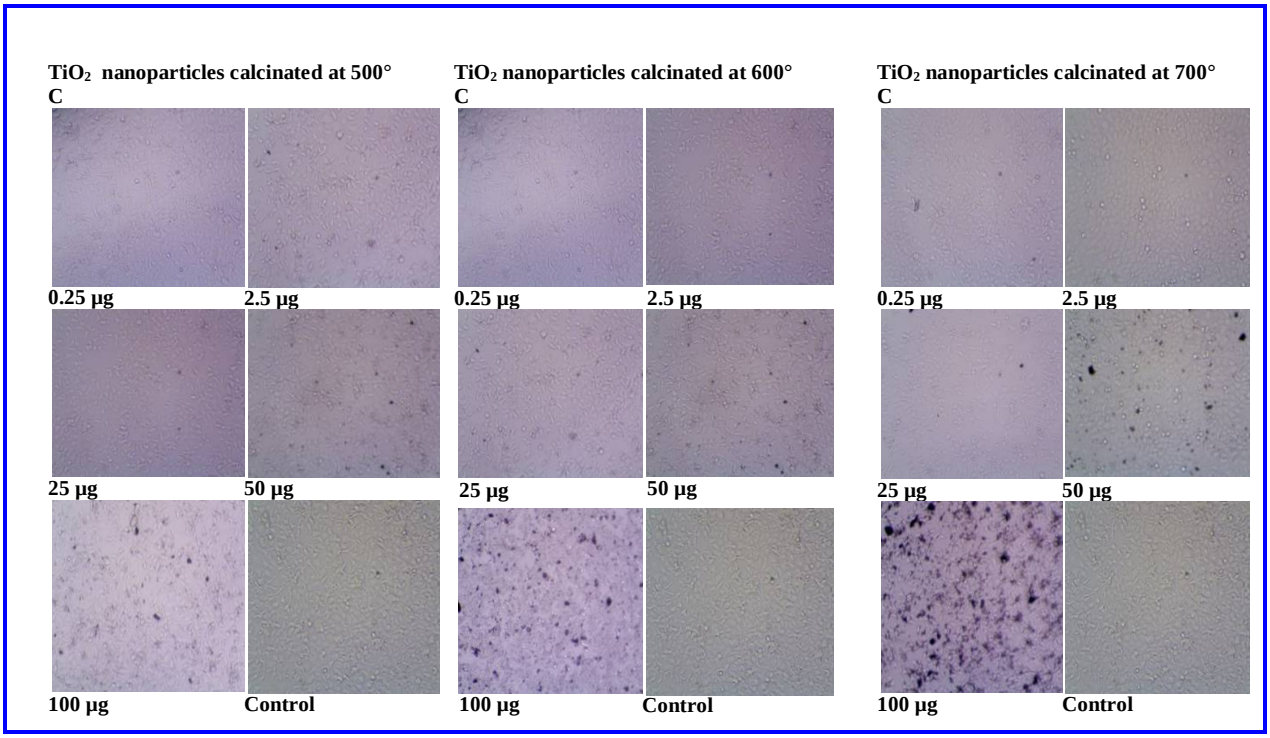

Fig. 9: Percentage inhibition of TiO_2 nanoparticles calcinated at 500° C, 600° C, 700° C

Table 1. Percentage of inhibition and IC50 value for different calcinated TiO_2 nanoparticles at various concentrations

Percentage inhibition of TiO_2 nanoparticles calcinated at 500° C

Conc (µg/ml)	% cell inhibition	IC50 value (µg)
0.25	0	

Percentage inhibition of TiO_2 nanoparticles calcinated at 600° C

Conc (µg/ml)	% cell inhibition	IC50 value (µg)
0.25	3.14	
2.5	2.31	

Percentage inhibition of TiO_2 nanoparticles calcinated at 700° C

Conc (µg/ml)	% cell inhibition	IC5 valu (µg
0.25	1.33	
2.5	4.54	

2.5	**1.2**	**>100**
25	**1.57**	
50	**3.59**	
100	**7.67**	
Control	**0.337**	

		>100
25	**3.21**	
50	**4.06**	
100	**13.4**	
Control	**0.337**	

		>100
25	**3.34**	
50	**5.02**	
100	**12.03**	
Control	**0.337**	

3.7 High Resolution Transmission Electron Microscope (HRTEM)

The HRTEM was used to confirm the distribution pattern, growth of prepared nanoparticles and also confirm the size of nano particles by directly measured from the ruler of the images. In general, TiO_2 nanoparticles have strong tendency to agglomerates to form a larger particle. The image 8 shows that most of the TiO_2 nanoparticles aggregates together and also spherical or nearly spherical and expand shaped particles with approximately uniform size of 35 nm to 50 nm. This exhibit lattice fringes which was used to calculate d-spacing and found to be 0.222 nm. This d-spacing value has been compared with standard JCPDS data corresponds to the plane (200) of anatase.

3.8 Cytotoxicity activity of TiO_2

The synthesised TiO_2 nanoparticles assessed cytotoxic effects after 48 h exposure and cisplatin was used as standard Mosmann *et al.* 1983; Monks *et al.* 1991;. Figure 8 shows the percentage inhibition of TiO_2 nanoparticles calcinated at 500° C, 600° C, and 700° C. The IC50 value is found greater than 100 µg/ml against human embryonic kidney cell line (HEK 293) for tested TiO_2 nanoparticles. This result indicates TiO_2 nanoparticles did not shows any cytotoxicity activity at the tested concentrations. Table 1 shows the % of inhibition and IC50 value for different calcinated TiO_2 nanoparticles at various concentrations. The tested TiO_2 nanoparticles low or did not show cytotoxicity activity against human cell line.

4. CONCLUSION

Titanium dioxide nanoparticles have been successfully synthesized by solgel method with using of hydroxylamine hydrochloride as a hydrolysis catalyst. From the XRD analysis, anatase phase was identified for TiO_2 nanoparticles calcinated at 500° C and 600° C for 5 h and converting it into rutile form when it is calcinated at 700° C for 5 h. TiO_2 nano particle size determined from Debye-Scherrer's formula is 30 nm, 37 nm and 47 nm. EDXAanalysis shows that no impurities are present in the prepared TiO_2 samples. UV-Visible spectrum of TiO_2 nanoparticles at three temperatures shows red shift in the absorbance edge and is due to the change in surface morphology, particles size.The band gaps of nanoTiO_2 measured by graphical method are 2.95 eV, 2.86 eV and 2.79 eV. Photoluminescence study indicates that the strong emission peaks obtained in 383 nm, 385 nm and 385 nm region confirm direct recombination between electrons in the conduction band and holes in the valence band. High Resolution Transmission Electron Microscope of TiO_2 nanoparticles shows aggregate together and also spherical or nearly spherical with approximately uniform size of 35 to 50 nm. FTIR spectrum analysis shows the peaks at 433 cm^{-1}, 514 cm^{-1} to700 cm^{-1} shows bending and stretching mode of Ti-O-Ti. The cytotoxicity activity results of TiO_2 at different temperatures show very small or no cytotoxicity activity.

REFERENCES

Akarsu, M., Asilturk, M., Sayilkan, F., Kiraz, N., Arpac, E., Sayilk, H., A Novel Approach to the Hydrothermal Synthesis ofanatase titania Nanoparticles and the Photocatalytic Degradation of Rhodamine B, *Turk. J. Chem.*, 30(3), 333-343(2006).

Byun, D., Kim, Y., Lee, K., Hofmann, P., Photocatalytic TiO_2 deposition by chemical vapor deposition, *Journal of Hazardous Materials*, 73(2), 199-206(2000). doi: 10.1016/S0304-3894(99)00179-X

Czanderna, W., Rao, C. N. R., Honig, J. M.,The anatase-rutile transition. Part 1.Kinetics of the transformation of pure anatase, *Trans.Faraday Soc.*, 54,1069(1958). doi: 10.1039/TF9585401069

Elangovan, S. V., Chandramohan, V., Sivakumar, N., Senthil, T. S., Synthesis and characterization of ZnO nanoparticles at different molarity concentrations for photocatalytic applications,*Desalination and water treatment*, 21, 1–8(2015). doi:10.1080/19443994

Hadjipanayis, G. C., Siegel, R.W., eds., *Nanophase Materials, Kluwer Academic Publishers, Dordrecht, NATO ASI Series*, 1994, pp.E 260.

Juergen, H., Braun, Baidins, A., Marganski, R. E., TiO_2 pigment technology: a review, *Progress in Organic Coatings*, 20(2), 105-138(1992). doi:10.1016/0033-0655(92)80001-D

Kamat, P.V., Photochemistry on nonreactive and reactive (semiconductor) surfaces, *Chem. Rev*., 93(1), 267-300(1999). doi:10.1021/cr00017a013

Kavan, L., Gratzel, M., Gilbert, S.E., Klemenz, C., Scheel, H., Electrochemical andPhotoelectrochemical Investigation of Single-Crystal Anatase, *J. Am. Chem. Soc*., 118(28), 6716-6723(1996). doi: 10.1021/ja954172l

Khan, A. M., Akhtar, S. M., Yang, O. B., Synthesis, characterization and application of sol–gel derived mesoporous TiO_2 nanoparticles for dye-sensitized solar cells, *Solar energy*, 84(12), 2195-2201(2010). doi:10.1016/j.solener.2010.08.008

Krol, R., Goossens, A., Schoonman, J., Schottky, M., Analysis of Nanometer-Scale thin-Film Anatase TiO_2, *J. Electrochem. Soc*., 144(5), 1723-1727(1997). doi:10.1149/1.1837668

Liqiang, J., Xianojun, S., Baiqi, X., Weimin, C., and Honggang, F., The preparation and characterization of La doped TiO_2 nanoparticles and their photocatalytic activity, *Journal of Solid State Chemistry*, 177, 3375-3382 (2004). doi:10.1016/j.jssc.2004.05.064

Mark, H. F., Othmer, H. F., Overberger, C. G., Seaberg G. T.,*Encyclopedia of Chemical Technology*, *John Wiley*, *New York*, 1983, pp.139.

Mogyorosi, K., Dekany, I., Fendler, J. H., preparation and characterization of clay mineral intercalated TiO_2 nanoparticle,*Lanqmuir*, 19(7), 2938(2003). doi:10.1021/la025969a

Monks, A., Scudiero, D., Skehan, P., Shoemaker, R., Paull, K., Vistica, D., Hose, C., Langley, J., Cronise, P., Wolff, A. V., Goodrich, M. G., Campbell, H., Mayo, J., Boyd, P., Feasibility of high flux anticancer drug screen using a diverse panel of cultured human tumour cell lines,*Journal of the National Cancer Institute*, 83, 757-766(1991). doi:10.1093/jnci/83.11.757

Mosmann, T., Rapid colorimetric assay for cellular growth and survival: application to proliferation and cytotoxicity assays,*Journal of Immunological Methods*, 65, 55-63(1983). doi:10.1016/0022-1759(83)90303-4

Navrotsky, A., Kleppla, O. J.,*Journal of the American Ceramic Society*, 50(11), 626- 630.

Prasad, K., Pinjari, D. V., Pandit, A. B., Mhaske, S. T., Phase transformation of nanostructured titanium dioxide from anatase-to-rutile via combined ultrasound assisted sol– gel technique, *Ultrasonics Sonochemistry*, 17(2), 409-415(2010). doi: 10.1016/j.ultsonch.2009.09.003

Rammal, A., Brisach, F., Henry, M., Chimie, C. R., Hydrothermal synthesis of TiO_2 anatasenanocrystals using hexaprismatic-shaped oxo-carboxylate complexes, *C. R. Chimie*, 5(1), 59-66(2002). doi:10.1016/S1631-0748(02)01292-4

Reidy, D. J., Holmes, J. D., Morris, M. A.,The critical size mechanism for the anatase to rutile transformation in TiO_2 and doped-TiO_2,*Journal of the European ceramic society*, 26(9), 1527(2006). doi:10.1016/j.jeurceramsoc.2005.03.246

Senthil, T. S., Kima, D., Muthukumarasamy, N., Kanga, M., Closely packed dense network rutile nanorods with gadolinium for efficient dye sensitized solar cells, *Applied Surface Science*, 313, 858–863(2014). doi:10.1016/j.apsusc.2014.06.090

Swapan, K., Das, Manas, K., Bhunia, and Bhaumik, A., Self-assembled TiO_2 nanoparticles: mesoporosity, optical and catalytic properties,*Dalton Trans.*, 39, 4382–4390(2010). doi: 10.1039/C000317D

Vijayalakshmi, R., and Rajendran, V.,Synthesis and characterization of nano-TiO_2 via different methods, *Arch. Appl. Sci. Res.*, 4(2), 1183-1190(2012).

Wang, D., Xiao, L., Luo, Q.,Li, X., An, J., Duan, Y., Highlyefficient visible light TiO_2 photocatalyst prepared by sol–gel method at temperatureslower than 300° C, *Journal of Hazardous Materials*, 192(1), 150-159(2011). doi: 10.1016/j.jhazmat.2011.04.110

Weast, R.,*C Hand book of Chemistry and Physics*, *CRC Press Boca RatonFL*, 1984.

Yoganarasimhan, S. R., Rao, C. N. R.,Mechanism of crystal structure transformations. Part 3.—Factors affecting the anatase-rutile transformation,*Trans. Faraday Soc.*, 58, 1579(1962). doi: 10.1039/TF9625801579

Yuan, S., Chen, S., Hu, S., Fabrication of TiO_2 nanoparticles /surfactant polymer complex film on glassy carbon electrode and its application to sensing trace dopamine, *Mat. Sci. Eng.C*, 25(4), 479- 485(2005). doi:10.1016/j.msec.2004.12.004

Zallen, R., Moret, M. P., The optical absorption edge of brookite TiO_2, *Solid state Communications*, 137(3), 154-157(2006). doi:10.1016/j.ssc.2005.10.024

Zhang, R., Gao, L., Zhang, Q., Photodegradation of surfactants on the nanosized TiO_2 prepared by hydrolysis of the alkoxide titanium, *Chemosphere*, 54(3), 405-411(2004). doi: 10.1016/S0045-6535(03)00588-5

Zhao, Y., Li, C. Z., Liu, X. H., Gu, F., Jiang, H. B., Shao, W., Zhang, L., and He, Y., Synthesis and optical properties of TiO_2 nanoparticles, *Material Letter*, 61(1), 79-83(2007). doi:10.1016/j.matlet.2006.04.010